Computational study of modification of cyanidin as high efficient organic sensitizer for dye sensitized solar cells

Kalpana Galappaththi[1], Piyasiri Ekanayake[1,3]*, Mohammad Iskandar Petra[2]

[1]Applied Physics Program, Faculty of Science, Universiti Brunei Darussalam, Jalan Tungku Link, Gadong, BE 1410, Brunei Darussalam
[2]Faculty of Integrated Technologies, Universiti Brunei Darussalam, Jalan Tungku Link, Gadong, BE 1410, Brunei Darussalam
[3]Physical and Geological Sciences Programme, Centre for Advanced Material and Energy Sciences, Universiti Brunei Darussalam, Jalan Tungku Link, Gadong, BE 1410, Brunei Darussalam

*corresponding author email: piyasiri.ekanayake@ubd.edu.bn

Abstract

This study reports the results of theoretical investigation of a newly designed cyanidin based molecular structure, (*P02*), as an efficient sensitizer for dye sensitized solar cells (DSSCs). To design the structure of *P02*, chemical structure of the widely used promising natural dye sensitizer cyanidin is combined with α-cyanocinnamic acid and the resultant structure is computationally simulated by using SPARTAN'10 software package. The molecular geometries, electronic structures, absorption spectra and deprotonation energies of newly designed organic sensitizer are investigated by employing density functional theory (DFT) and time-dependent density functional theory (TDDFT) approaches using GAUSSIAN'09W software package. As a reference, DFT and TDDFT calculations are also performed on the structure of cyanadin. The solvation effect of these dyes in ethanol are included in all calculations. The computational studies on the new dye revealed that the broadening of the absorption spectra in visible region with significant shifting towards a longer wavelength region compared to the cyaniding dye, indicating that the new dye *P02* should exhibit better performances as a sensitizer in DSSCs due to its improved photon absorbtion properties.

Index Terms: density functional theory, absorption spectra, dye sensitized solar cells, cyanadin

1. Introduction

One of the current global challenge is to meet the increasing global energy consumption without effecting the environment. In this sense solar energy provides clean abundant energy and is therefore an excellent candidate for a future environmentally friendly energy source. Solar cells are devices that are able to convert solar energy into electrical energy.

The aim of solar cell research is to increase the solar energy conversion efficiency at low cost to provide a cost-effective sustainable energy source. Among the solar cells known today, dye sensitized solar cells (DSSCs), developed in 1991 by Grâtzel and coworkers in Switzerland are one class of a cost-effective and environmentally friendly solar cells.[1-8] These DSSCs mainly comprise with a nano structured high band gap semiconducting electrodes combined with efficient electron injection dyes. The sensitizing dye in DSSCs is mainly responsible for the capture of sunlight. To improve its efficiency, dye sensitizer should have a broad absorption spectrum as much as possible to match with large range of photons available in solar energy.[9] Therefore, the synthetic dyes used in DSSCs with higher efficiencies consist with rare earth materials and complexed structures, eventually increasing the cost of these devices. Therefore, one of the possible alternatives to replace these expensive dyes with rare earth materials is the usage of natural dyes in these
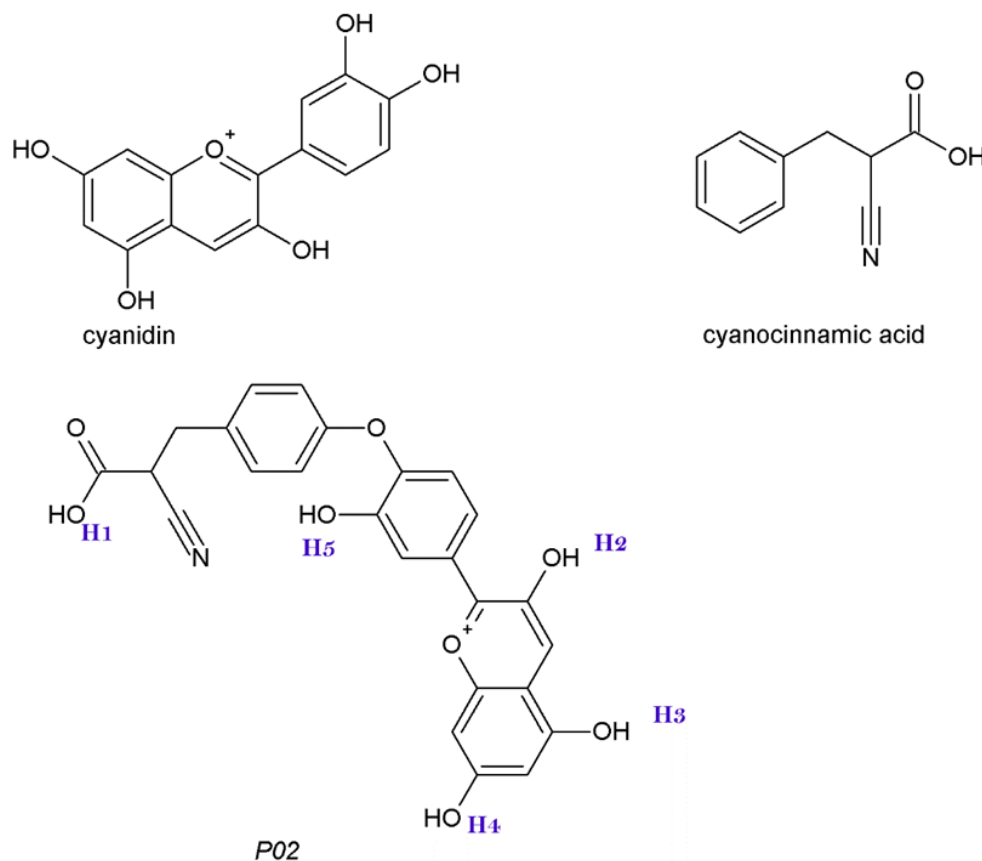
Figure 1. Fundamental molecular structure of cyanidin, cyanocinnamic acid and newly designed *P02*.

DSCSs which effectively reduce the cost and the hazardness to the environment.[10-16]

However, the reported efficiencies of DSSCs employing with natural dyes are still very poor mainly due to their poor light harvesting properties associated with them. Therefore, to improve the efficiencies of these devices with natural dyes, the dye sensitizer should have a broad absorption spectrum as much as possible to match with large range of photon energies available in the solar energy spectrum.[9] Most of the natural dyes available consist of cyanidin as the main active component of the dye and strongly absorbs around 500 nm wavelength. Therefore, synthesis of cyanidin based new dyes, having the ability to capture of more photons would be an efficient approach to solve this problem. However, before synthesizing these new dyes it is worth of finding out whether these new dyes would really show the desirable optical properties such as positions of the bands, energy gaps, etc. Hence in this study a cyanidin based organic dye

is designed and computationally characterized to be used as a novel sensitizer in DSSCs, by attaching one hydroxyl group on benzene ring of cyanidin is attached–to the benzene ring of α-cyanocinnamic acid unit as shown in **Figure 1**.

2. Computational studies
The molecular structures of *P02* and cyanidin are computed using Spartan'10 software[17] to retrieve the molecular geometric coordinates. Both density functional theory (DFT) and time-dependent density functional theory (TDDFT) calculations are performed using Gaussian'09W software.[18] The geometry of P02 and cyanidin in ground state is fully optimized using the Becke's three parameters Lee-Yang-Parr hybrid functional (B3LYP).[19] In the calculations 6-31g (d) basis set is adopted to describe metal free atoms. All the calculations are computed including solvation effect of these molecules in ethanol. The models of electron density of various energy levels of the *P02* are visualized using GaussView Version 5.0. The deprotonation energies of *P02* are calculated

Table 1: Summary of DFT computational calculation of the structures of cyanidin and *P02* in ethanol, with and without geometrical optimization

Sensitizer	Solvent Effect	Without geometric optimization			With geometric optimization		
		HOMO (eV)	LUMO (eV)	Energy gap (eV)	HOMO (eV)	LUMO (eV)	Energy gap (eV)
Cyanidin	Ethanol	-6.91	-3.82	3.10	-6.18	-3.39	2.79
P02	Ethanol	-5.31	-3.90	1.41	-6.48	-3.66	2.82

using B3LYP hybrid functional and 6-31g (d) basis set in vacuum condition.[20]

3. Results and discussion
DFT calculation
Table 1 summarizes the results obtained from repeated DFT calculations on *P02* molecule with solvent effect in ethanol for the geometrically optimized structure. The estimated electron energy values of the main two important levels i.e., highest occupied molecular orbital level (HOMO), lowest unoccupied molecular level (LUMO) and the band gap values are tabulated for both without optimized and optimized structures. It is observed that the data, especially the band gap value of *P02*, obtained after geometrical optimization in ethanol is nearly equal to band gap value of cyanidin in ethanol.

The electron injection from the excited dye molecule to the conduction band of TiO_2 is more efficient if the LUMO level is higher than conduction band edge of TiO_2. For efficient regeneration of the oxidized dye molecule to its original state by the hole conductor, the energy difference between HOMO level and energy level of redox couples must be sufficiently high. Further, the LUMO level must be above the conduction band of TiO_2 while HOMO level must be below the energy level of redox couple.[21]

The HOMO and LUMO energy levels of *P02* and cyandin, as calculated from DFT are plotted with respect to energy in vacuum level in ***Figure 2*** and the superimposed on the plots are the energy levels corresponding to the conduction band of TiO_2 and the redox couple.[22] The results in ***Figure 2*** show that the *P02* satisfy the conditions for photo-energy conversion.

The HOMO level is a core factor of electron donor mechanism. The electron donating capability will increase when HOMO level is more negative. According to our computational results, energy levels of HOMO of cyanidin and *P02* in ethanol with geometric optimization are -6.18eV and -6.48eV, respectively, revealing that the HOMO level of *P02* is -0.3eV more negative than that of cyaniding. Hence *P02* has more electron donating ability to the HOMO level of the dye molecule with compared to that of cyanidin.
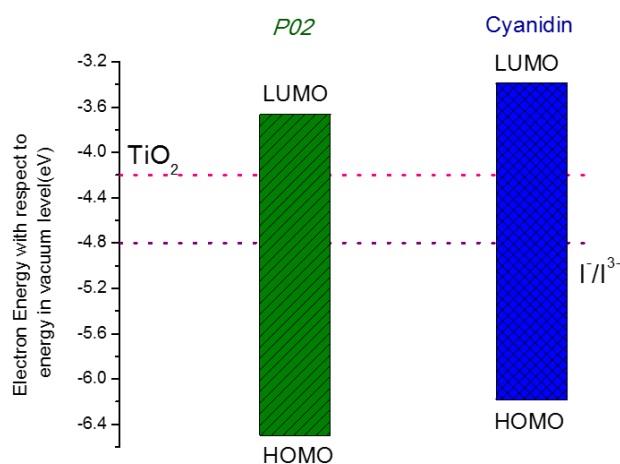

Figure 2. Energy level diagram showing HOMO, LUMO energy levels of *P02* and cyanidin, redox potential and conduction band of TiO_2. Computational results of HOMO and LUMO are obtained using B3LYP/6-31g (d) level and with geometric optimization in ethanol.

TDDFT and Optical Properties
To gain insight of the excitation energy, electronic transition, optical properties and UV/Vis absorption spectra for the singlet to singlet transition of newly designed dye *P02* and our reference dye cyanidin are simulated using TDDFT with hybrid functional B3LYP in ethanol solution. The lowest five singlet-singlet excitations are included in TDDFT calculation.

Table 2: Computed excitation energies in (eV), (nm) and the oscillator strength (f) of the cyanidin and *P02* obtained by TDDFT calculations at B3LYP/6-31g (d) level with the inclusion of geometric optimization under the solvation effect of ethanol.

Sensitizer	Optimized, in ethanol			
	Calculated Energy		Oscillator strength	MO configuration
	(eV)	(nm)	(f)	(coefficient)*
Cyanidin	2.52	492.16	0.583	HOMO-> LUMO = 0.695
	2.82	439.86	0.010	HOMO-3-> LUMO = 0.318 HOMO-2 ->LUMO= 0.467 HOMO ->LUMO+1 = 0.211
	3.17	391.21	0.273	HOMO-3->LUMO = 0.322 HOMO-2->LUMO = 0.192 HOMO-1->LUMO = 0.586
	3.88	319.36	0.025	HOMO-4->LUMO = 0.687
	4.49	276	0.055	HOMO-3->LUMO = 0.516
P02	2.45	506.25	0.397	HOMO->LUMO = 0.681
	2.60	476.52	0.08	HOMO-1->LUMO = 0.653 HOMO->LUMO= 0.176
	2.86	433.73	0.068	HOMO-2->LUMO = 0.685 HOMO-1->LUMO = 0.150
	3.20	387.20	0.416	HOMO-3->LUMO= 0.676 HOMO-1->LUMO = 0.140
	3.53	351.72	0.000	HOMO-4->LUMO = 0.706

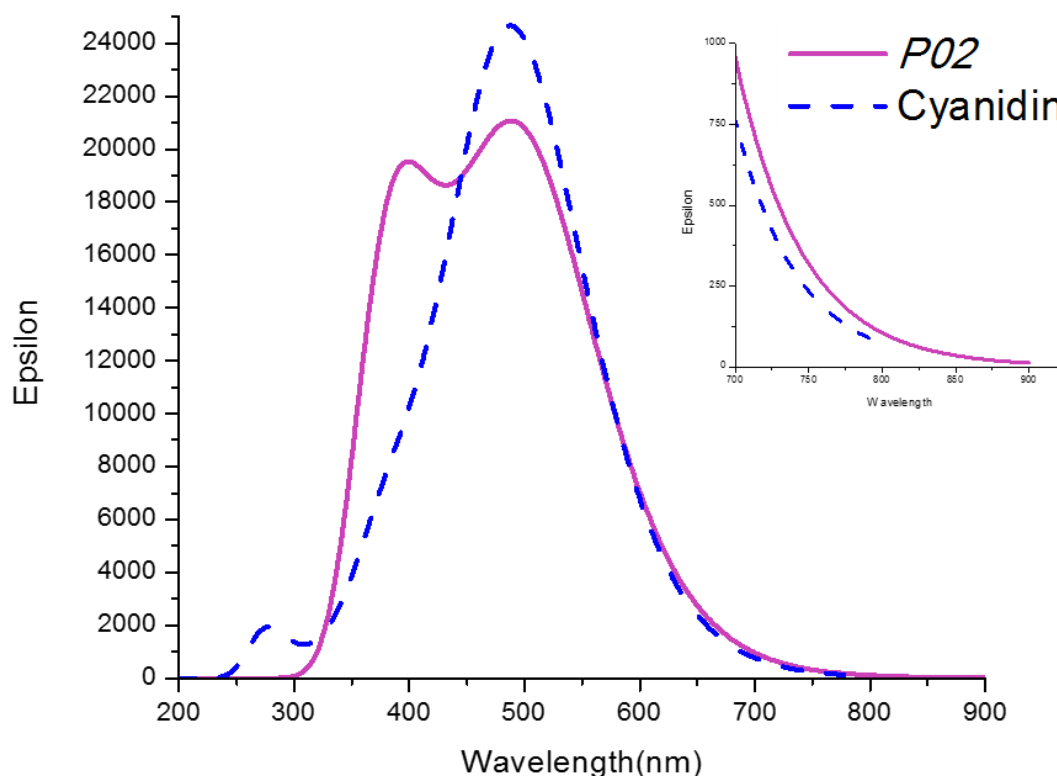* Molecular orbital with configuration coefficient <0.1 are not shown.

Figure 3. UV-vis absorption spectra obtained for the *P02* and Cyanidin via output of TDDFT calculations with solvation effect of ethanol solution. Inset shows an enlarged absorption spectra in 700 nm to 900 nm range.

The excitation energy, oscillator strength, configuration and molar extinction coefficient for the five states of *P02* and cyanidin dye are calculated using B3LYP on 6-31g (d) basis set are shown in ***Table 2*** and the computer simulated UV-vis absorption spectra obtained for the *P02* and cyanidin via TDDFT calculations are shown in ***Figure 3***.

Oscillator strength expresses the strength of transition to the excited states. The higher the oscillator strength, the higher the possibility of the molecule as a sensitizer.[23-25] At the first excitation state, the oscillator strength of *P02* and cyanidin are 0.397 and 0.583, respectively, and the transition is HOMO to LUMO. The maximum absorption wavelength, λ_{max}, of *P02* and cyanidin are at 506.25 nm and 492.16 nm, respectively (***Table 2***) and the corresponding energies are 2.45 eV and 2.52 eV.

At the second excitation state, the oscillator strength for the *P02* and cyanidin are 0.08 and 0.01, respectively. At this excitation state *P02* involved HOMO-1 to LUMO transition, whereas cyanidin involved HOMO – 2 to LUMO transition. The calculated energy of *P02* and cyanidin are 2.60 eV and 2.82 eV and λ_{max} are at 476.52 nm and 439.86 nm.

At the third excitation state, the *P02* and cyanidin showed 0.068 and 0.273 oscillator strength. If excitation occur at this state, the *P02* and cyanidin would displayed HOMO – 2 to LUMO and HOMO – 1 to LUMO transitions, respectively. The λ_{max} of the *P02* and cyanidin are at 433.73 nm and 391.21 nm and their corresponding energies are at 2.86 eV and 3.17 eV.

At the forth excitation state, the *P02* and cyanidin showed 0.416 and 0.025 oscillator strength. If excitation occur at this state, the *P02* and cyanidin would displayed HOMO – 3 to LUMO and HOMO – 4 to LUMO transitions, respectively. The λ_{max} of the *P02* and cyanidin are at 387.20 nm and 319.36 nm and their corresponding energies are at 3.20eV and 3.88 eV.

At the fifth excitation state, the oscillator strength for *P02* is zero and cyanidin showed 0.055 oscillator strength. If excitation occur at this state, the *P02* and cyanidin would have displayed HOMO – 4 to LUMO and HOMO – 3 to LUMO transitions, respectively. The λ_{max} of the *P02* and cyanidin are at 351.72 nm and 276 nm and corresponding energies are at 3.53eV and 4.49 eV.

P02 has produced four significant oscillator strengths up to the forth excitation states, while cyanidin only produced three significant oscillator strength at the first, third and fifth excitation states. This suggested that *P02* has more ability to sensitize the semiconductor in DSSC than the cyanidin. In addition, the λ_{max} values of the *P02* at each five excitation states shifted to longer wave lengths compared to λ_{max} of cyanidin by 14.09 nm, 36.66 nm, 42.52 nm, 67.84 nm and 75.72 nm, respectively. Also, the absorption spectra of the *P02* is broader compared to cyanidin (***Figure 3***) indicating its ability to absorb more energy. The absorption spectrum of *P02* is significantly broader at shorter wavelengths of the visible region.

Molecular Electronic Structure
Modelling of the electron density clouds behavior at the transition of various energy levels corresponding to first five excited states of *P02* is shown in ***Figure 4*** to ***Figure 8***. At different energy levels, it could be observed that electron density clouds are localized at different regions of the *P02* molecule.

P02 molecule consist of cyanidin and α-cyanocinnamic acid. One hydroxyl group on benzene ring of cyaniding is attached to benzene ring of α-cyanocinnamic acid unit. Almost all the ground state energy levels such as HOMO-4, HOMO-3, HOMO-2, HOMO-1and HOMO levels of *P02* are π-type. At the HOMO level the electron density cloud is mostly localized in the α-cyanocinnamic acid unit and the benzene ring of cyanidin. Negligible amount of electron cloud is observed on chromenylium unit, whereas the electron density cloud of the HOMO-1 are delocalized over the entire molecule of *P02*. The HOMO-2 and HOMO-3 of *P02* have similar
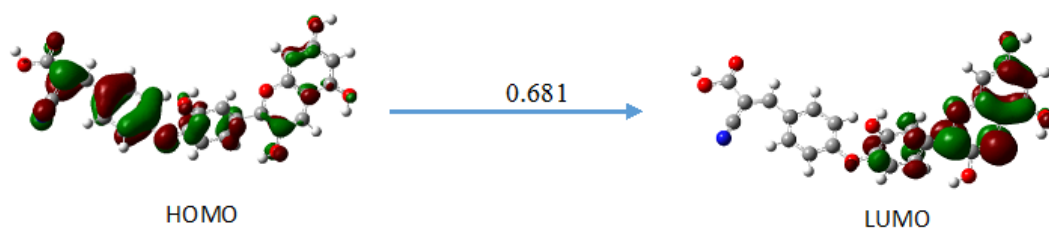
Figure 4. The electron transition for the 506.25 nm absorption of P02 in ethanol under the TDDFT calculation with isovalue of contour = 0.03.
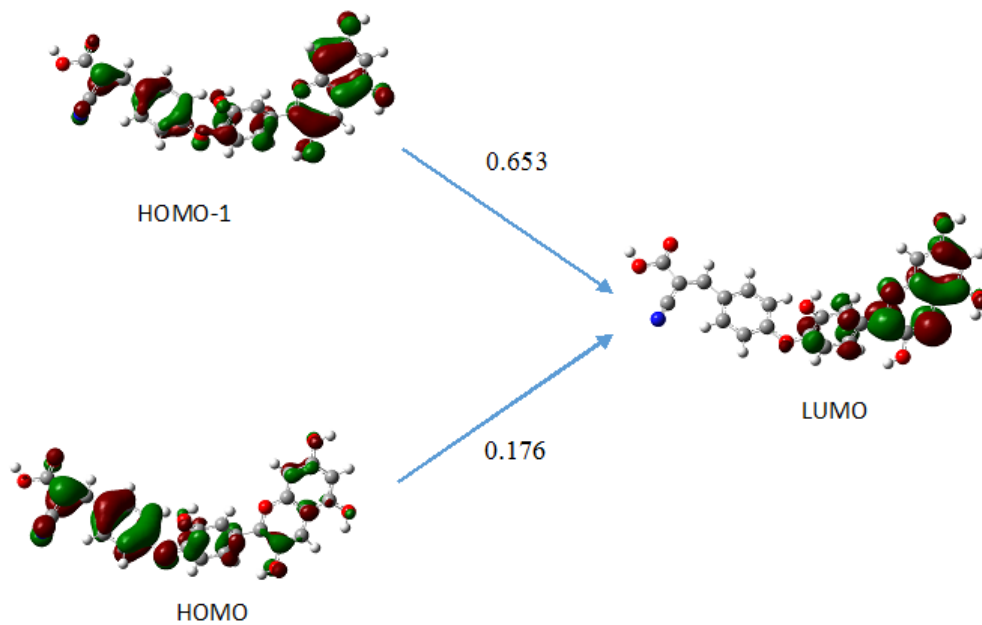

Figure 5. The electron transition for the 476.52 nm absorption of P02 in ethanol under the TDDFT calculation with isovalue of contour = 0.03.
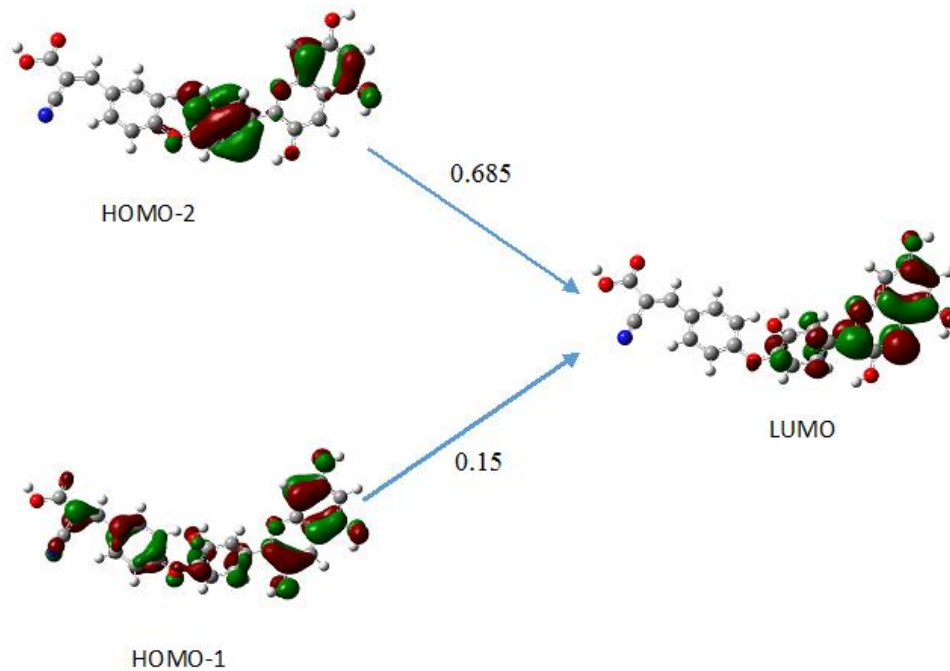

Figure 6. The electron transition for the 433.73 nm absorption of P02 in ethanol under the TDDFT calculation with isovalue of contour = 0.03.
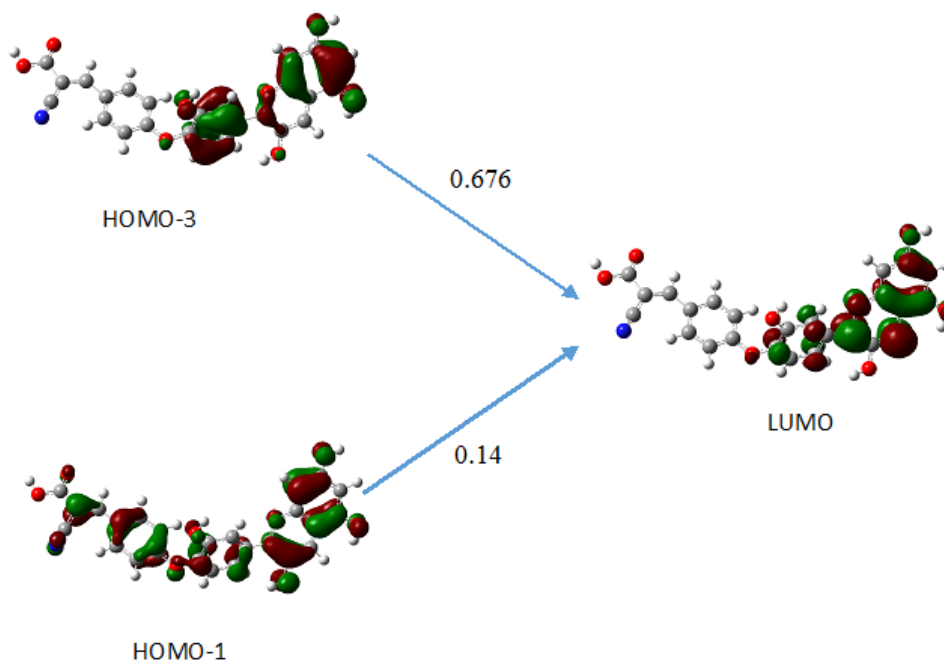
Figure 7. The electron transition for the 387.2 nm absorption of P02 in ethanol under the TDDFT calculation with isovalue of contour = 0.03.
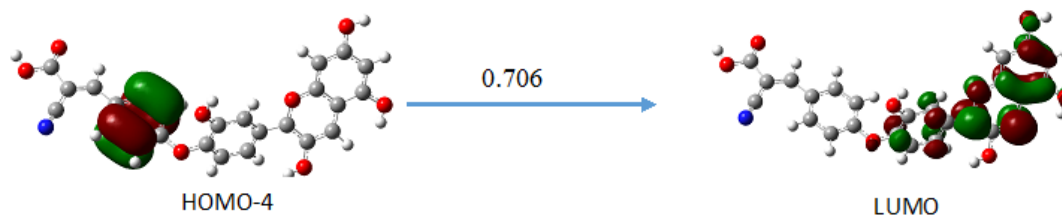

Figure 8. The electron transition for the 351.72 nm absorption of P02 in ethanol under the TDDFT calculation with isovalue of contour = 0.03.

electron density cloud patterns as electron clouds are localized over two benzene rings in cyanidin unit of *P02*. At HOMO-4, dense π type electron density cloud observed on benzene ring of α-cyanocinnamic acid unit.

In the *P02* molecule, the electron cloud of LUMO is π^* type and the molecular orbital is localized at cyanidin unit. At LUMO the electron density cloud localized in cyanidin unit. Here the electron density cloud is observed to be denser in chromenylium unit than the benzenedial in cyanidin unit of *P02*. The photogenerated electrons are excited to chromenylium unit on electrode of TiO₂. Subsequently, electrons are easily injected into the conduction band of TiO₂. This electron injection is most possible from the chromenylium unit as it has denser electron density cloud in the LUMO π^* state. Therefore,

the anchoring groups of *P02* molecule that may efficiently inject electrons into the TiO_2 are deduced to be the hydroxyl groups H2, H3, H4 and H5 (**Figure 1**).

Proton affinity

Deprotonation energy is calculated by the energy difference between the optimized protonated and deprotonated *P02* dye molecule in B3LYP/6-31g (d) level of theory under vacuum condition[19, 20], as shown in **Table 3**. The common anchoring group of natural dyes are the hydroxyl (–OH) group and the carboxyl group (–COOH).[20] The *P02* molecular structure contains four hydroxyl groups and one carboxyl group. H1 (see **Figure 1**) has shown the highest deprotonation energy while H4 has shown the smallest deprotonation energy. The descending order of the deprotonation energies are H1 > H2 > H3 > H5 > H4. The difference in

Table 3. Single deprotonation energies (kJ mol^{-1}) of the *P02* sensitizer.

Sensitizer	Deprotonation energies (kJ mol^{-1})				
	-H1$^+$	-H2$^+$	-H3$^+$	-H4$^+$	-H5$^+$
P02	283.4	250.5	236.5	232.2	233.0

deprotonation energy between H1 and H4 is 51.2 kJ mol^{-1}. The lowest value of the deprotonation energy indicates the most probable group that could anchor onto TiO$_2$.[26, 27] Therefore, from the results of these calculations, we can deduce that the most possible anchoring group of *P02* is H4. When the three most probable anchoring groups H3, H4 and H5 are compared, electron density cloud localization, calculated from TDDFT, only occurs on H3 and H4, but not on H5, deducing H3 and H4 as the most beneficial anchoring groups of *P02*.

4. Conclusions
The molecular geometries, electronic structures, absorption spectra and deprotonation energies of newly designed molecule of *P02* sensitizer are investigated by using DFT and TDDFT computational calculations. By evaluating HOMO and LUMO energy levels, obtained from DFT calculations of geometrically optimized structure of *P02* molecule with solvent effect in ethanol, it was revealed that *P02* satisfies main requirement for an efficient electron injection with the LUMO level of P02 higher than the conduction band of the TiO$_2$ and the HOMO level of *P02* sufficiently lower than the redox couple. Furthermore, the *P02's* HOMO energy level is -0.3eV more negative than cyanidin's HOMO energy level. Hence *P02* has more electron donating ability with compared to that of cyanidin. The UV-vis absorption spectra revealed that the *P02* complex exhibits broader absorption indicating its ability to absorb wider energy range in the visible region.

Though there is a carboxyl group in *P02*, the electron affinity calculations reveal that it has the highest deprotonation energy compared to the hydroxyl groups indicating its lowest possibility to anchor onto TiO$_2$. The most probable anchoring groups are H4 and H5 and H3, in the descending order. In addition, at the excited states the electron clouds are localized towards the hydroxyl groups, especially H4 and H3, in the cyanidin unit of *P02*.

All these results suggest the more promising sensitization ability of *P02* which is designed by modifying the sensitizer cyanidin.

References
[1] P. Ekanayake, M.R.R. Kooh, N.T.R.N. Kumara, A. Lim, M.I. Petra, N.Y. Voo, C.M. Lim, *Chemical Physics Letters*, **2013**, 585, 121-127.
[2] B. O'Regan, M. Grätzel, *Nature*, **1991**, 353,737–740.
[3] Tennakone, K., et al., *Journal of Photochemistry and Photobiology A: Chemistry*, **1996**, 94(2-3), 217-220.
[4] Calogero, G., et al., *International Journal of Molecular Sciences*, **2010**, 11(1), 254-267.
[5] Polo, A.S. and N.Y. Murakami Iha, *Solar Energy Materials and Solar Cells*, **2006**, 90(13), 1936-1944.
[6] Hagfeldt, A., et al., *Chemical Review*, **2010**, 110, 6595-6663.
[7] Polo, A.S., M.K. Itokazu, and N.Y. Murakami Iha,. *Coordination Chemistry Reviews*, **2004**, 248(13-14), 1343-1361.
[8] Smestad, G.P. and M. Gratzel, *Journal of Chemical Education*, **1998**, 75(6), 752.
[9] Siriporn Jungsuttiwong , Ruangchai Tarsang, Taweesak Sudyoadsuk, Vinich Promarak, Pipat Khongpracha, Supawadee Namuangruk, *Organic Electronics,* **2013**, 14,711–722
[10] Narayan, M.R., *Renewable and Sustainable Energy Reviews*, **2012**, 16(1), 208-215.
[11] Fernando, J.M.R.C. and G.K.R. Sendeera, *Current Science*, **2008**, 95(5), 4.
[12] Calogero, G., et al., *Solar Energy*, **2012**, 86(5), 1563-1575.
[13] A. Lim, N. Haji Manaf, K. Tennakoon, R.L.N. Chandrakanthi, L.B.L. Lim, J.M.R.S.

Bandara, P. Ekanayake, *Journal of Biophysics*, **2015** ,8.

[14] A. Lim, N.T.R.N. Kumara, A.L. Tan, A.H. Mirza, R.L.N. Chandrakanthi, M.I. Petra, L.C. Ming, G.K.R. Senadeera, P. Ekanayake, *Spectrochimica Acta Part A: Molecular and Biomolecular Spectroscopy*, **2015**, 138, 596-602.

[15] N.T.R.N. Kumara, P. Ekanayake, A. Lim, M. Iskandar, C.M. Lim, *Journal of Solar Energy Engineering*, **2013**, 135, 031014-031014.

[16] A. Lim, D.N.F.B. Pg Damit, P. Ekanayake, *Ionics*, **2015**, 21, 2897-2904.

[17] B. Deppmeier, A. Driessen, T. Hehre et al., "*Spartan'10,*" Wavefunction, **2011**.

[18] M. J. Frisch, G. W. Trucks, H. B. Schlegel et al., "*Gaussian 09,*" Revision C.01, Gaussian,Wallingford, Conn, USA, **2010**.

[19] C. Lee, W. Yang, R.G. Parr, *Physical Review*, **1988**, B 37,785.

[20] C. Qin, A.E. Clark, *Chemical physics letters*, **2007,** 438, 26-30.

[21] G. Calogero et al., *Photochem. Photobiol. Sci.*, **2013**, 12, 883.

[22] H.C. Chu et al., *Dyes Pigments*. **2012**, 93, 1488-1497.

[23] F. De Angelis, S. Fantacci, A. Selloni, M.K. Nazeeruddin, M. Gratzel, *J.Phys. Chem. C*, **2010**, 114, 6054-6061.

[24] F. De Angelis, S. Fantacci, A. Selloni, M.K. Nazeeruddin, M. Gratzel, *J. Am, Chem. Soc.* **2007**, 129, 14156-14157.

[25] N. T. R. N. Kumara, Muhammad Raziq Rahimi Kooh, Andery Lim, et al., *International Journal of Photoenergy*, **2013**, Article ID 109843.

[26] T.R. Heera, L. Cindrella, *J. Mol. Model.* **2010**, 16, 523.

[27] Ming-Jing Zhang, Yuan-Ru Guo, Gui-Zhen Fang, Qing-Jiang Pan, *Computational and Theoretical Chemistry*, 2013**,** 1019, 94-100.